Microfabrication by plasma etching

- Introduction to plasma etching
- Surface reactions
- Etching process
- Application

- quartz crystal microbalance

- References

Prof. M.A.M. Gijs, Dr. V.K. Parashar, Swiss Federal Institute of Technology Lausanne (EPFL) 2021

Introduction

- Dry or plasma etching : a family of methods by which a solid state surface **is etched in the gas phase**
  - **physically**, by ion bombardment
  - **chemically**, by a reaction with reactive species
  - by a **combined physical-chemical** mechanism
- Two major classes:
  - **Glow discharge techniques**: plasma is generated in the same vacuum chamber as the substrate.
  - **Ion-beam techniques**: plasma is generated in a separate chamber, ions are extracted and directed towards the substrate.

- **Isotropic and anisotropic** dry etching processes exist for single crystalline, polycrystalline and amorphous films.
- **Selectivity of a dry etch**: difference in etch rate between mask and film to be etched.
  - At low pressure (10^{-3}-10^{-4} Torr), obtaining anisotropic etching is easy, having selectivity is difficult.
  - At high pressure (1 Torr), chemical effects dominate, which means better selectivity and isotropic etching profiles.

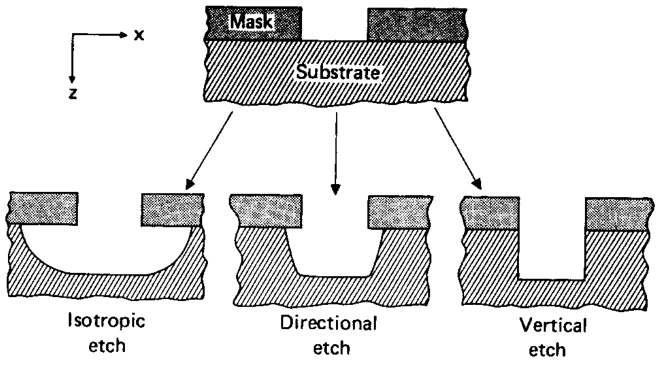

FIGURE 2.2 Directionality of etching processes.

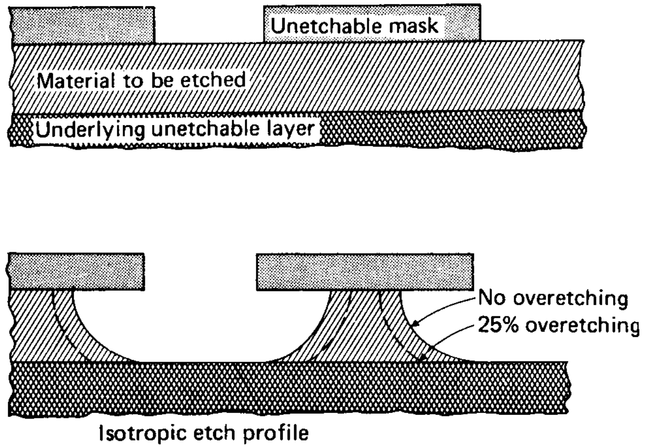

FIGURE 2.3 Example illustrating the loss of dimensionality incurred by an isotropic etch when the etch depth is of the order of the lateral dimensions involved. Making the initial lithography smaller compensates for the loss of dimensionality by overetching.

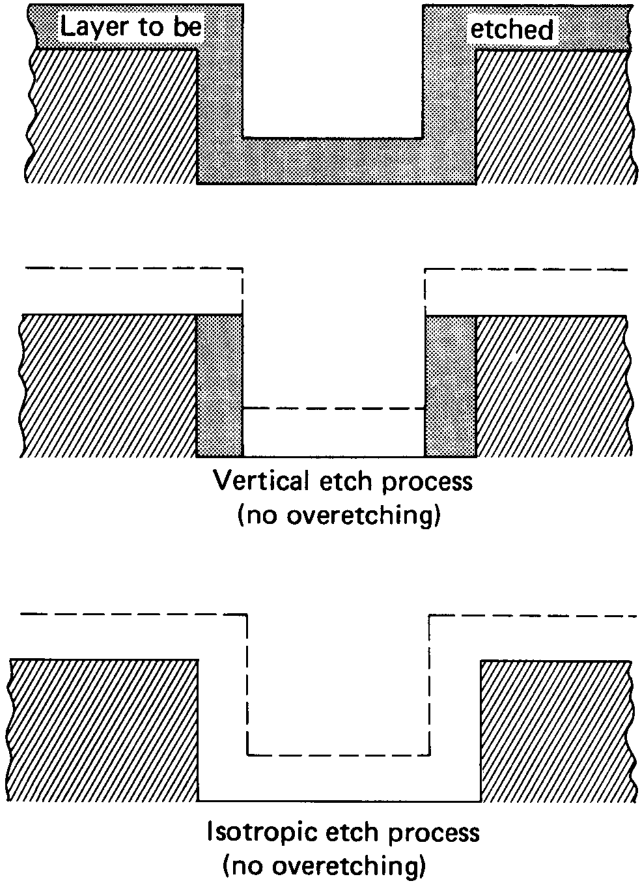

FIGURE 2.4 An example of dry etching illustrating a case where an isotropic etch is preferred to a vertical etch process. To clear the layer on the vertical walls, an isotropic etch only requires a minimal overetch while an anisotropic etch requires a substantial amount of overetching.

DC plasma etching

- Bombarding energy of ions is proportional to the **DC voltage** difference between plasma and the surface.
- Substrate is on the cathode in Ar plasma and sufficiently energetic ions (200-1000 eV) will induce physical etching. Due to collisions with other gas species, ions lose energy. This gives dependence on pressure.

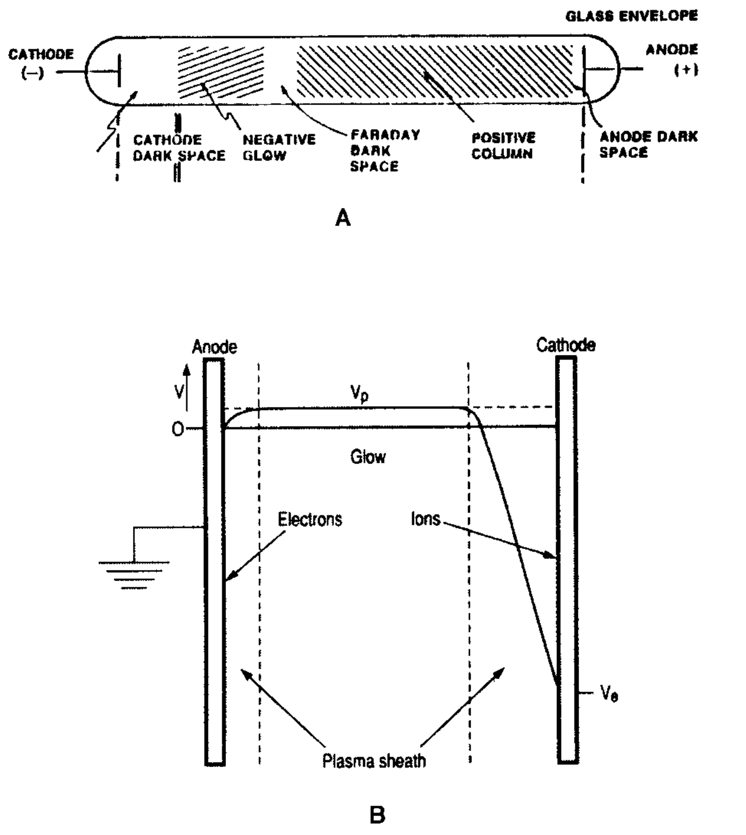

FIGURE 2.6 Glow discharge in a DC diode system. (A) Structure of the glow discharge in a DC diode system. (B) Voltage distribution in a DC diode discharge in equilibrium.

Effect of plasma pressure

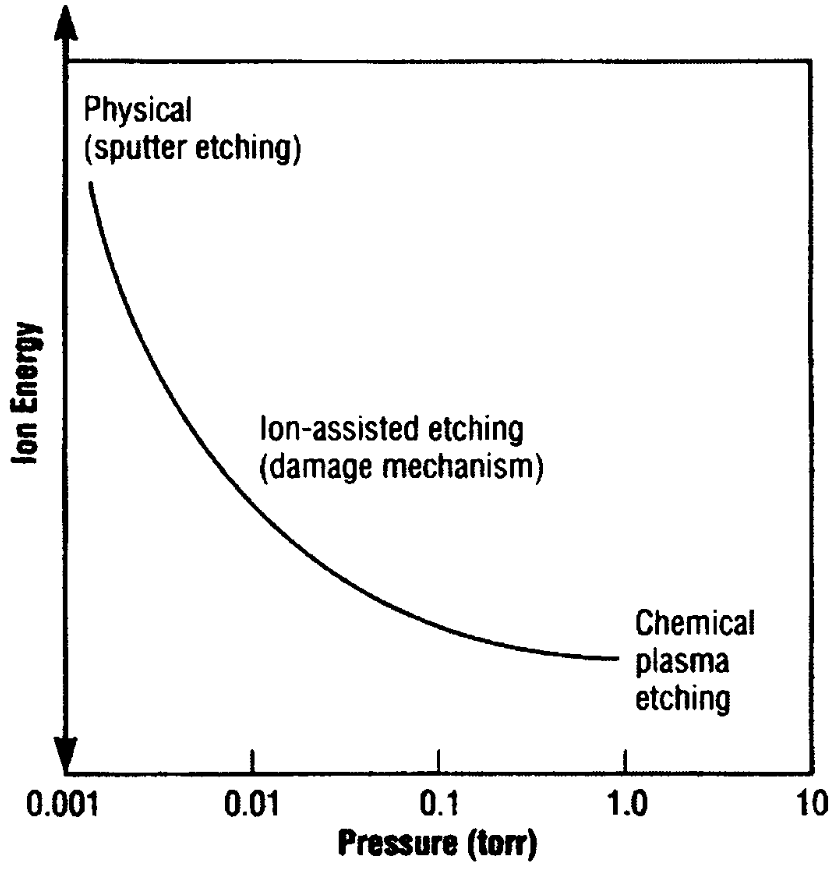

FIGURE 2.14 Ion energy vs. pressure for a plasma. (From Flamm, D. L., *Solid State Technol.*, 35, 37–39, 1991. With permission.)

RF plasma etching

- **Radio frequent (RF) voltage**, e.g. at 13.56 MHz, is applied between two electrodes; power of a few kW.
- RF plasma allows to etch dielectrics as well as metals.
- Substrates are laid at the cathode of a reactor at 10^{-1}-10^{-2} Torr Ar.
- Ionisation degree of plasma:10^{-4}-10^{-6}.

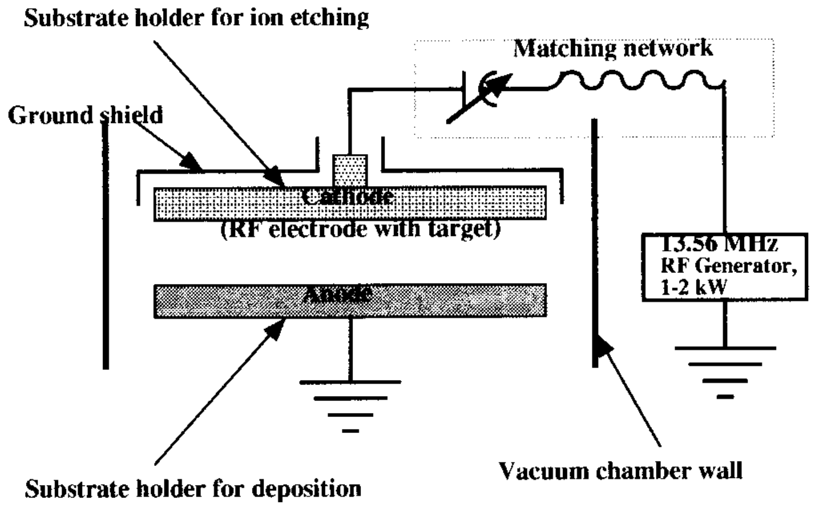

FIGURE 2.8 Two electrode set-up (diode) for RF ion sputtering or sputter deposition. For ion sputtering, the substrates are put on the cathode (target); for sputter deposition, the substrates to be coated are put on the anode.

Sputtering or ion etching

- Impinging ions erode or sputter etch the substrate by **momentum transfer**.
- *Advantages*:
  - volatility of etching products is not critical, **hence no large difference in etching rates** for different materials
  - directional **anisotropy** process
- *Disadvantages*:
  - **masking** is sometimes problem
  - high gas pressure needed to obtain large currents, hence short mean free path of electrons → considerable **redeposition of sputtered atoms** on etched surface.
  - Electrical damage from ion bombardment and implantation of substrate.

Dry chemical etching

- **Reaction mechanism**
  - Production of reactive species in the gas-phase. For example, CF_4 gas dissociates by impact with 1-10 eV electrons. Reactive species such as CF_3^+, CF_3, and F are formed.
  - Reactive species diffuse to the solid.
  - Reactive species adsorb on the substrate.
  - Reactive species diffuse over the surface and react with it.
  - Reaction products leave by desorption.
  - Reaction products diffuse away.
- The reaction with the smallest rate constant determines the overall reaction rate.

Physical-chemical etching

- 4 types of ion-surface interactions may promote dry etching
  - direct reactive ion beam etching (RIBE)
  - ion bombardment induces a reaction by making the surface more reactive for the neutral plasma species
  - ions clear the surface of film-forming reaction products
  - ion bombardment supplies the energy to drive surface reactions

Energy-driven anisotropy

- Ion bombardment disrupts unreactive substrate and causes damage such as dangling bonds or dislocations, resulting in a reactive substrate.
- This type of etching is **reactive ion etching (RIE)**, when it involves reactive chemicals in a diode reactor, and as **chemically assisted ion-beam etching (CAIBE)** when it involves a triode set-up.
- Etch rate in RIE is higher than without chemical component.
- *Example* :
  - Si etch rate in Ar sputtering : 10 nm/min
  - Si etch rate in CCl_2F_2 : 200 nm/min

Inhibitor-driven anisotropy

- Etching leads to production of **surface covering agent**, while ion bombardment clears the 'passivation' from horizontal surfaces.
- Protective film can originate from involatile etching products, for example formed from starting gases BCl_3, or freons (CCl_4 and CF_2Cl_2).
- *Example* : Si etching

  Adding H_2 to the CF_4 gas decreases etching rate, because fluorine reacts with H so that carbon compounds polymerise.

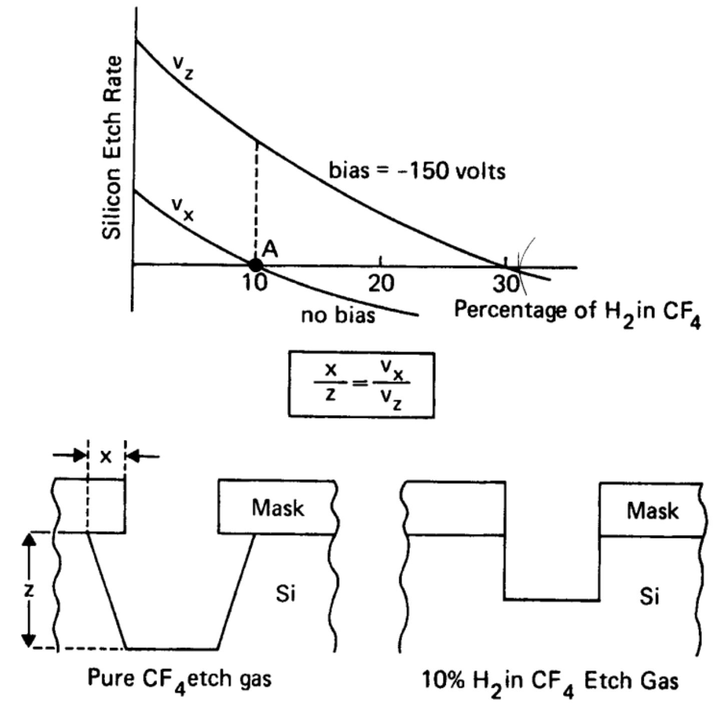

FIGURE 2.18 Trench profile manipulation by decreasing the fluorine-to-carbon ratio (through hydrogen introduction).[8]

New plasma sources

- Very **<u>high plasma densities</u>** produced by **microwave electron cyclotron resonance (ECR)** sources and **inductively coupled plasma (ICP)** sources.
- **ECR source**

  2.45 GHz microwave excitation resonating at the orbital frequency of e^- is coupled into the etching chamber, which is in a magnetic field generated by solenoid coils. A high-density plasma, maintainable at low pressure (10^{-5}-10^{-2} Torr), is produced.
- **ICP source**

  Plasma is driven inductively using standard 13.56 MHz radiation. Ion-producing electrons are coupled to the magnetic field generated by the RF source. Si etch rates : 6 μm/min, Si:SiO_2 selectivity 150:1 at – 100°C.

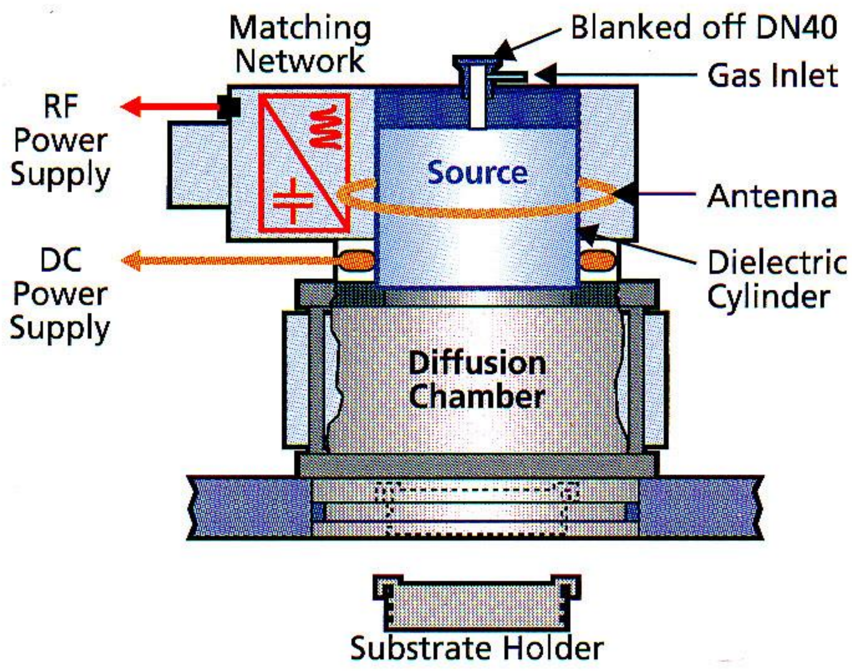

Fig. 5 Alcatel Process Chamber and ICP Source

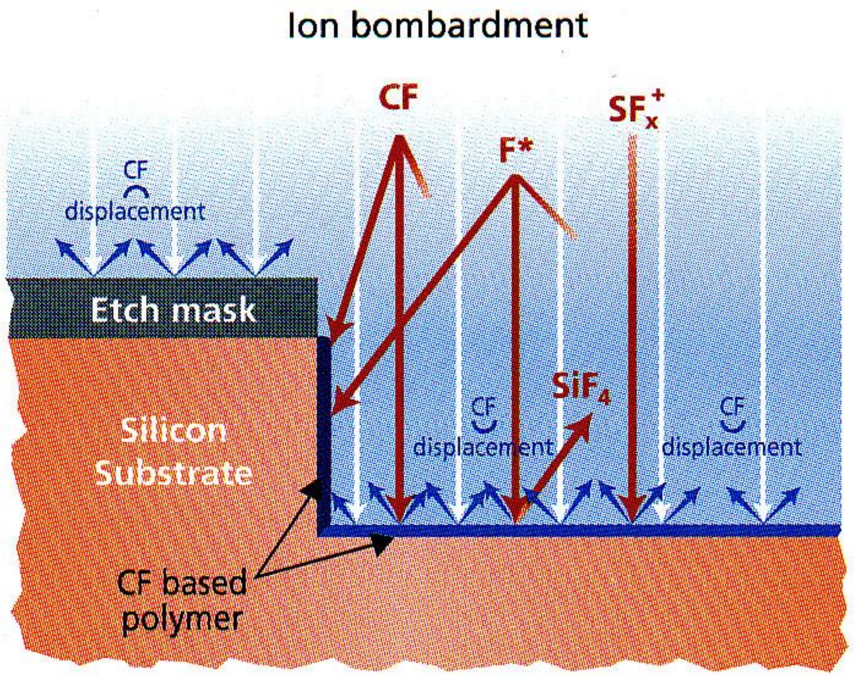

Fig. 4 Bosch Process

Bosch process

- Alternative etching steps (SF_6) and passivation steps by CF polymer forming gas (C_4F_8)
  - Etch rate : 10 μm/min
  - 150 mm diam. Si substrates
  - good uniformity
  - aspect ratio : 90 :1

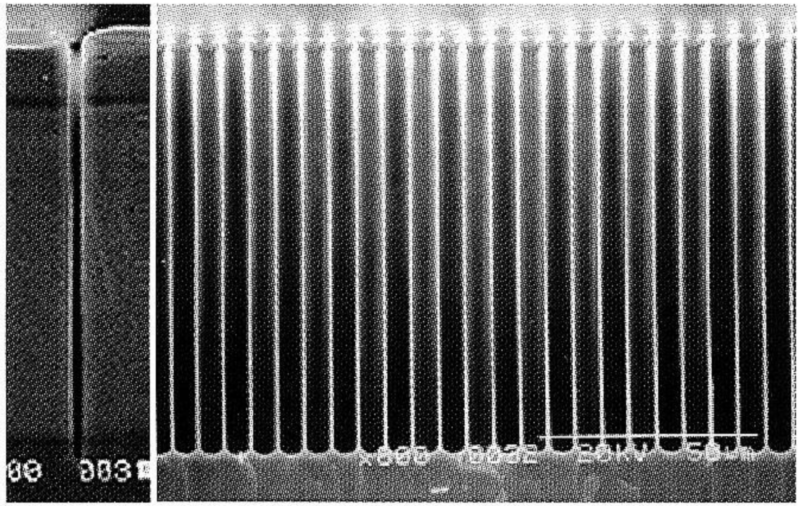

Fig. 3 High Aspect Ratio Etching using the A601E DRIE Etcher

Prof. M.A.M. Gijs, Dr. V.K. Parashar, Swiss Federal Institute of Technology Lausanne (EPFL) 2021

Si etching using the Bosch process

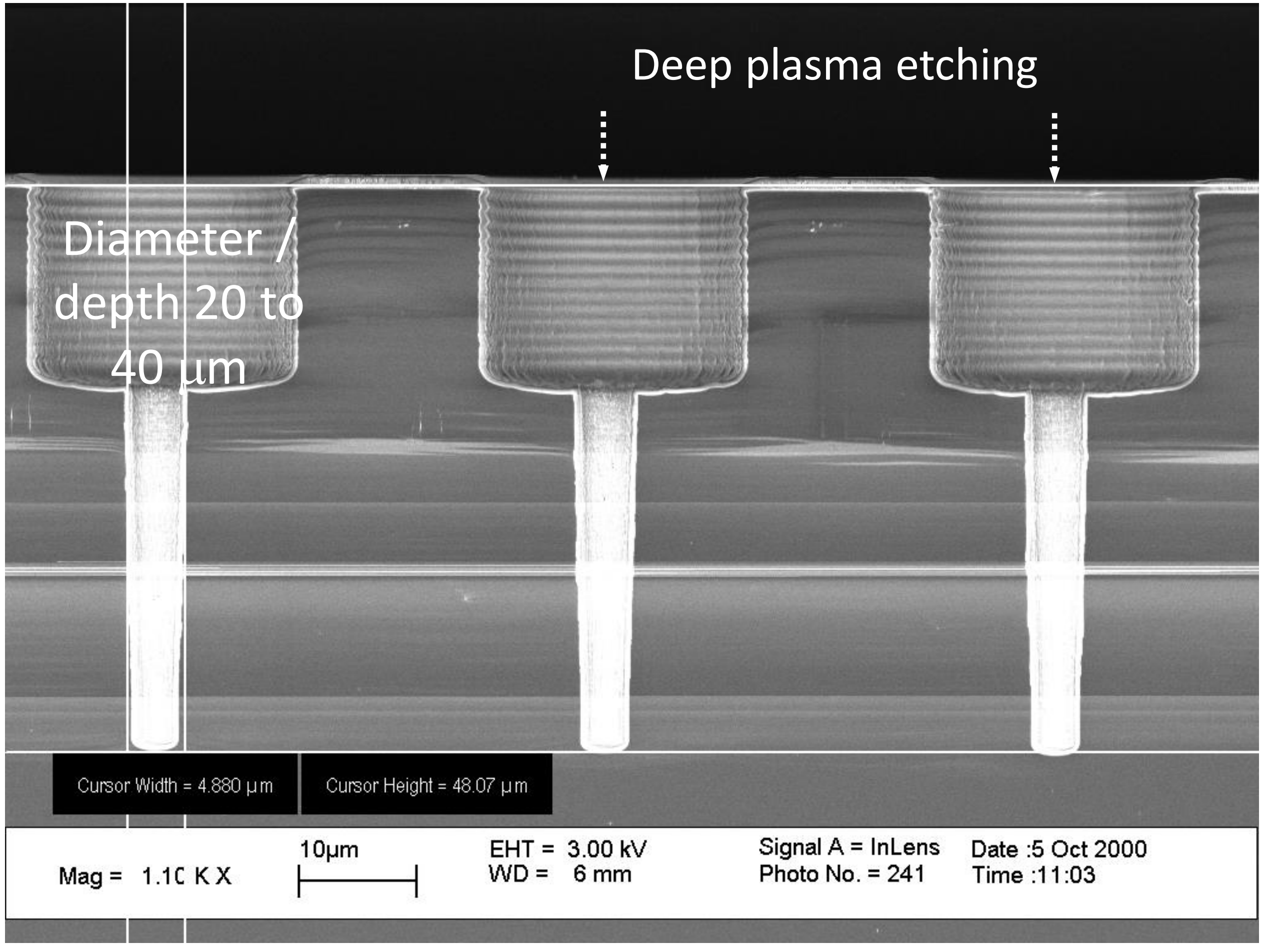

Surface reactions (C_xF_y plasma)

1. Adsorption of neutrals
2. Ion beam mixing and subsequent ion-enhanced chemical etching/sputtering
3. Pure chemical or thermal etching
4. Physical sputtering and direct ion deposition
5. Ion-enhanced deposition or neutral stiching by ions

Fundamental research done by studying the effect of well-defined ion beams

Sputtering and direct deposition coefficients

TABLE I. Physical sputtering and direct deposition coefficients of Ar^+, C^+, and CF_x^+ ions.

Ion	Substrate	Sputtering coefficient A [Eq. (7)]	Deposition coefficient A_d [Eq. (8)] or A [Eq. (9)]	Sputtering energy threshold (eV)	References/comments
Ar^+	Si	0.0337	...	20	14, 20, 50
CF_3^+	Si	0.0414±0.0019	A_d=0.0171, A=0.0414	74	40 for total yield. Threshold same as for SiO_2 from Ref. 47
CF_2^+	Si	0.0362±0.0014	A_d=0.0150, A=0.0362	200	40
CF^+	Si	0.1022±0.0067	A_d=0.0370, A=0.1022	777	40, $E<1000$ eV
C^+	Si	0.0490	A_d=0.0280, A=0.0490 $E_{\text{maximum deposition yield}}=800$ eV	2000	40
Ar^+	SiO_2	0.0139	...	18	14, 20, 50
CF_3^+	SiO_2	0.0456±0.0016	A_d=0.0189, A=0.0456	20	49, 48
CF_2^+	SiO_2	0.0306±0.0016	A_d=0.0127, A=0.0306	80	0.67×A of CF_3^+
CF^+	SiO_2	0.0228±0.0016	A_d=0.0094, A=0.0228	150	0.5×A of CF_3^+

Gogolides et al., J. Appl. Phys. 88, 5570 (2002)

Example of Si and SiO_2 etching trends

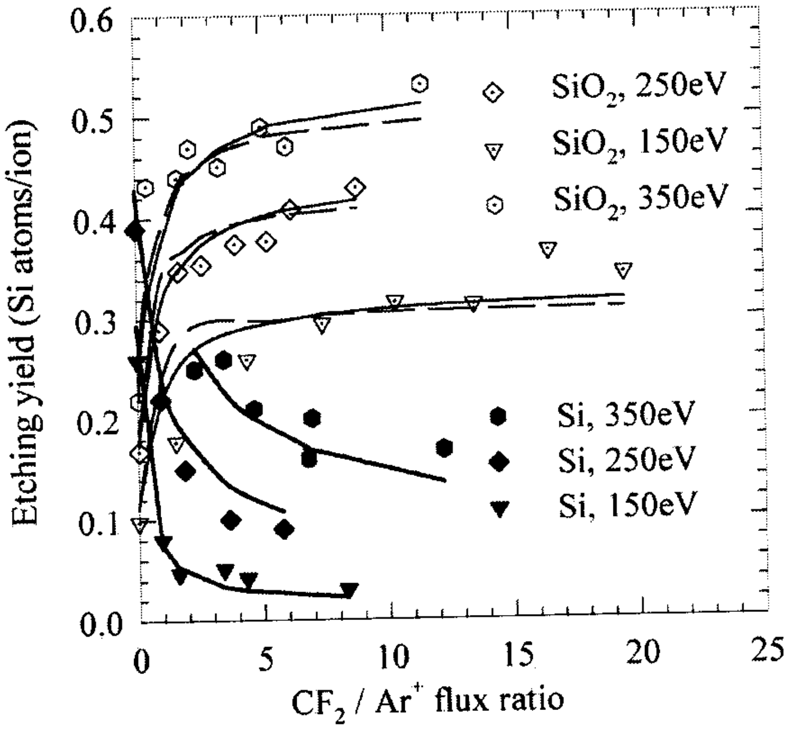

FIG. 1. Si and SiO_2 etching yield vs CF_2/Ar^+ flux ratio. Data from Gray *et al.* (see Ref. 20). Symbols: experiments at 150, 250, and 350 eV, thick solid lines: Fits for Si, thin solid lines: Fits for SiO_2 with a constant sticking coefficient for $CF_2(s_{CF_2})$, Dashed line: Fits for SiO_2 with a sticking coefficient increasing with ion energy. This fit is used to determine (1) the sputtering yield of carbon on SiO_2, (2) the ion-enhanced deposition yield (stitching) from fluorocarbon radicals, (3) the ion-enhanced etching of SiO_2 with CF_2 radicals.

Gogolides et al., J. Appl. Phys. 88, 5570 (2002)

Si etching reactions in fluorocarbon plasma

TABLE VII. Reaction set for Si etching in fluorocarbon plasma.[a]

	Reaction			Process	Flux dependency	Surface coverage	Rate coefficient
Physical sputtering							
(1)	Si^* $E>E_{th}$	→	$Si(g)+Si^*$	Physical sputtering	j_{ION}	$1-\theta_{TOT}$	y_{SP}
Reactions with fluorine atoms							
(2)	$2F(p)+Si^*$	→	$Si{-}F_2(s)$	F chemisorption	j_F	$1-\theta_{TOT}$	s_F
(3)	$Si{-}F_2(s)+2F(p)$	→	$SiF_4(g)+2Si^*$	Ion-enhanced chemical etching by F atoms	j_{ION}	θ_F	β'_F
(4)	$Si{-}F_2(s)$	→	$SiF_2(g)+2Si^*$	Ion-enhanced chemical sputtering	j_{ION}	θ_F	$\beta'_F b$
(5)	$Si{-}F_2(s)+2F(p)$ or $2F(g)$	→	$SiF_4(g)$	Thermal etching by F atoms	j_F	$1-\theta_{CF_x}-\theta_P$	$K(T)$
Reactions with CF_x $(x=1-3)$ or other fluorocarbon radicals							
(6)	$Si^*+CF_x(g)$	→	$Si{-}CF_y(s)$	Chemisorption of CF_x/partial dissociation	j_{CF_x}	$1-\theta_{TOT}$	s_{CF_x}
(7)	$Si{-}CF_y(s)$	→	$CF_y(g)+Si^*$	C sputtering	j_{ION}	θ_{CF_x}	y_C
(8)	$Si{-}CF_y(s)+F(p)$ or $F(g)$	→	$Si^*+CF_{y+1}(g)$	Recombination of CF_x with F	j_F	θ_{CF_x}	k_{REC}
Reactions of polymer creation or loss							
(9)	CF_x^+ at $E<E_{th1}$	→	Polymer P	Direct ion deposition (instead of sputtering)	j_{ION}	1	y_d
(10)	$Si{-}CF_x(s)$ at $E<E_{th2}$	→	Polymer P	Ion-enhanced deposition of sorbed radicals (stitching)	j_{ION}	θ_{CF_x}	β_s
(11)	$P{-}F(s/P)$	→	Polymer etch products	Ion-enhanced etching of polymer by sorbed F	j_{ION}	$\theta_{F/P}$	$\beta_{F/P}$
(12)	$P{-}CF_x(s/P)$ at $E<E_{th2}$	→	More polymer	Ion-enhanced deposition (stitching) of sorbed radicals	j_{ION}	$\theta_{CF_x/P}$	β_s

[a]p stands for physisorbed atoms. s stands for chemisorbed atoms or radicals, s/P stands for chemisorbed atoms or radicals on polymer surface and the (*) denotes a dangling bond or a site for chemisorption.

Gogolides et al., J. Appl. Phys. 88, 5570 (2002)

SiO$_2$ etching reactions in flu

TABLE VIII. Reaction set for SiO$_2$ etching in fluorocarbon plasmas.[a]

Reaction		Process	Flux dependency	Surface coverage	Rate coefficient
Physical sputtering					
(1) O_2–Si*	→ Si(g)+2O(g)+O_2–Si*	Physical sputtering	j_{ION}	$1-\theta_{TOT}$	y_{SP}
Reactions with F atoms					
(2) O_2–Si*(s)+2F(p)	→ O_2–Si–F_2(s)	Adsorption	j_F	$1-\theta_{TOT}$	s_F
(3) O_2–Si–F_2(s)+2F(p)	→ Si–F_4(g) +O_2(g)+2O_2–Si*	Ion-enhanced chemical etching by F	j_{ION}	θ_F	β'_F
(4) O_2–Si–F_2(s)	→ Si–F_2(g) +O_2(g)+2O_2–Si*	Ion-enhanced chemical sputtering	j_{ION}	θ_F	$\beta'_F b$
(5) O_2–Si–F_2(s)+2F(p) or 2F(g)	→ Si–F_4(g)+O_2(g)	Thermal etching by F	j_F	$1-\theta_{CF_x}-\theta_p$	K(T)
Reactions with CF_x $(x=1-3)$ or other fluorocarbon radicals					
(6) Si–O_2^*(s)+CF_x(g)	→ Si–O_2–CF_x(s)	Chemisorption	j_{CF_x}	$1-\theta_{TOT}$	s_{CF_x}
(7) 2Si–O_2–CF_x(s)	→ SiF_x(g)+2CO_2(g) +Si–O_2^*	Ion-enhanced chemical etching by CF_x radicals	j_{ION}	θ_{CF_x}	β_c
(8) Si–O_2–CF_x(s)	→ Si(s)+2COF$_x$(g) +Si–O_2^*	C sputtering	j_{ION}	θ_{CF_x}	y_C
(9) Si–O_2–CF_x(s)+F(p) or F(g)	→ Si–O_2+CF_{x+1}(g)	Recombination of CF_x with F	j_F	θ_{CF_x}	k_{REC}
Reactions of polymer creation or loss					
(10) CF_x^+ at $E<E_{th}$	→ polymer P	Direct ion deposition	j_{ION}	1	y_d
(11) Si–O_2–CF_x(s) at $E<E_{th}$	→ polymer P	Ion-enhanced deposition (stitching) of sorbed radicals	j_{ION}	θ_{CF_x}	β_s
(12) P–F(s)	→ etching of polymer	Ion-enhanced etching of polymer by F atoms	j_{ION}	$\theta_P\theta_{F/P}$	$\beta_{F/P}$
(13) P–CF_x(s)	→ more polymer	Ion-enhanced deposition of sorbed radicals (stitching)	j_{ION}	$\theta_P\theta_{CF_x/P}$	β_s

[a]p stands for physisorbed atoms, s stands for chemisorbed atoms or radicals, s/P stands for chemisorbed atoms or radicals on polymer surface, the (*) denotes a dangling bond or a site for chemisorption.

Gogolides et al., J. Appl. Phys. 88, 5570 (2002)

Etching process

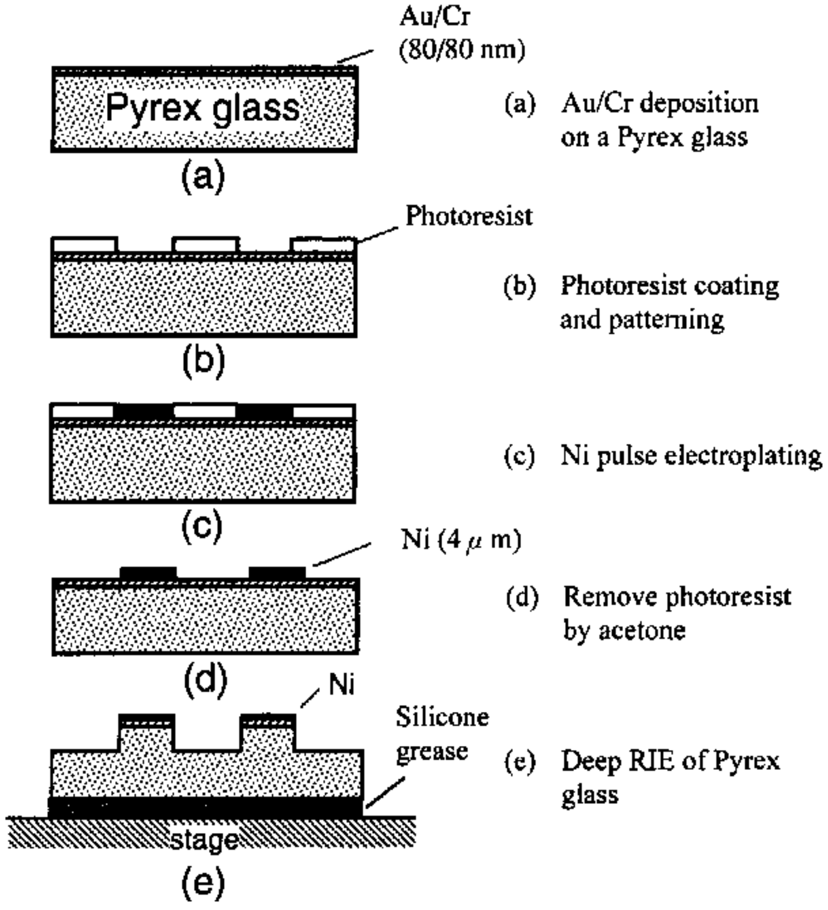

Fig. 2. Deep RIE process of Pyrex glass.

Example

- Electroplating of Ni mask
- Pulse plating of Ni : low internal stress and high purity (pulse interval 10 ms)
- Etching selectivity Ni:Pyrex = 14 - 20 (SF_6, p = 0.2 Pa, self-bias = -390 V)

Li et al., Sens. & Act. A 87, 139 (2001)

Influence of pressure

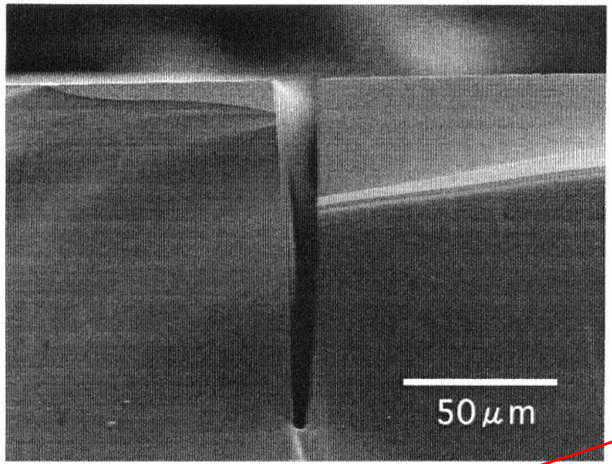

Fig. 1. A SEM micrograph of Deep RIE of Pyrex glass at the small mask opening width (10 μm in size).

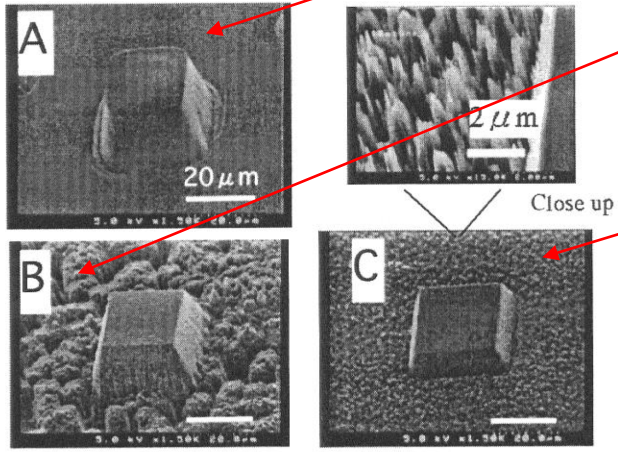

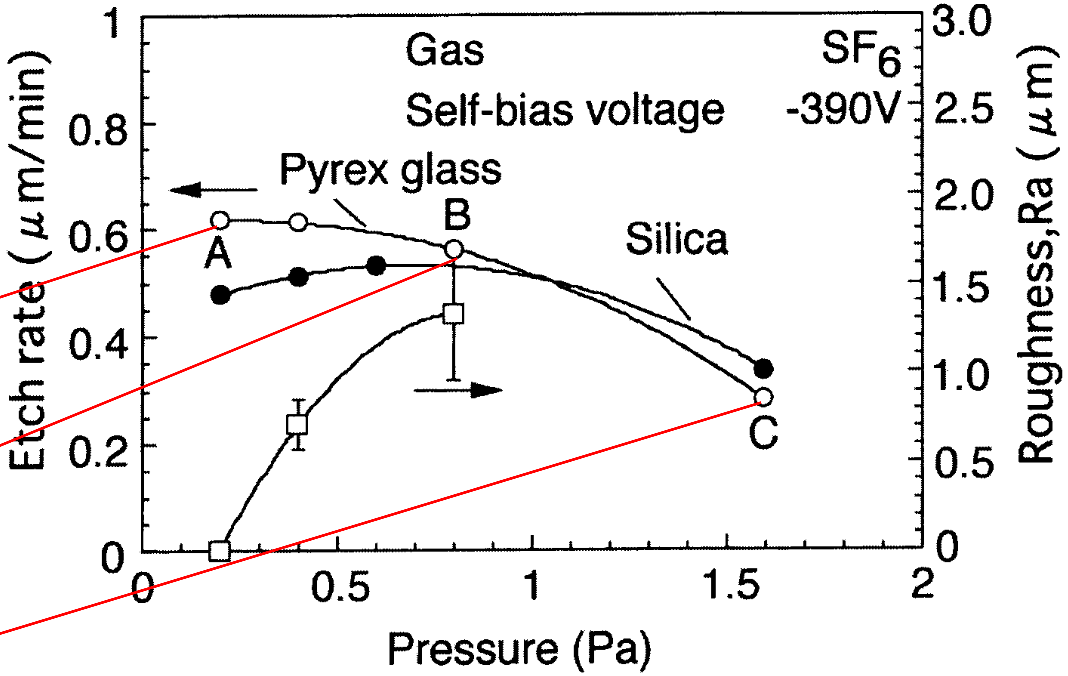

Fig. 3. Etch rates as a function of process pressure and the SEM images (self-bias voltage −390 V, etching time 1 h).

Li et al., Sens. & Act. A 87, 139 (2001)

Influence of self-bias

Li et al., Sens. & Act. A 87, 139 (2001)

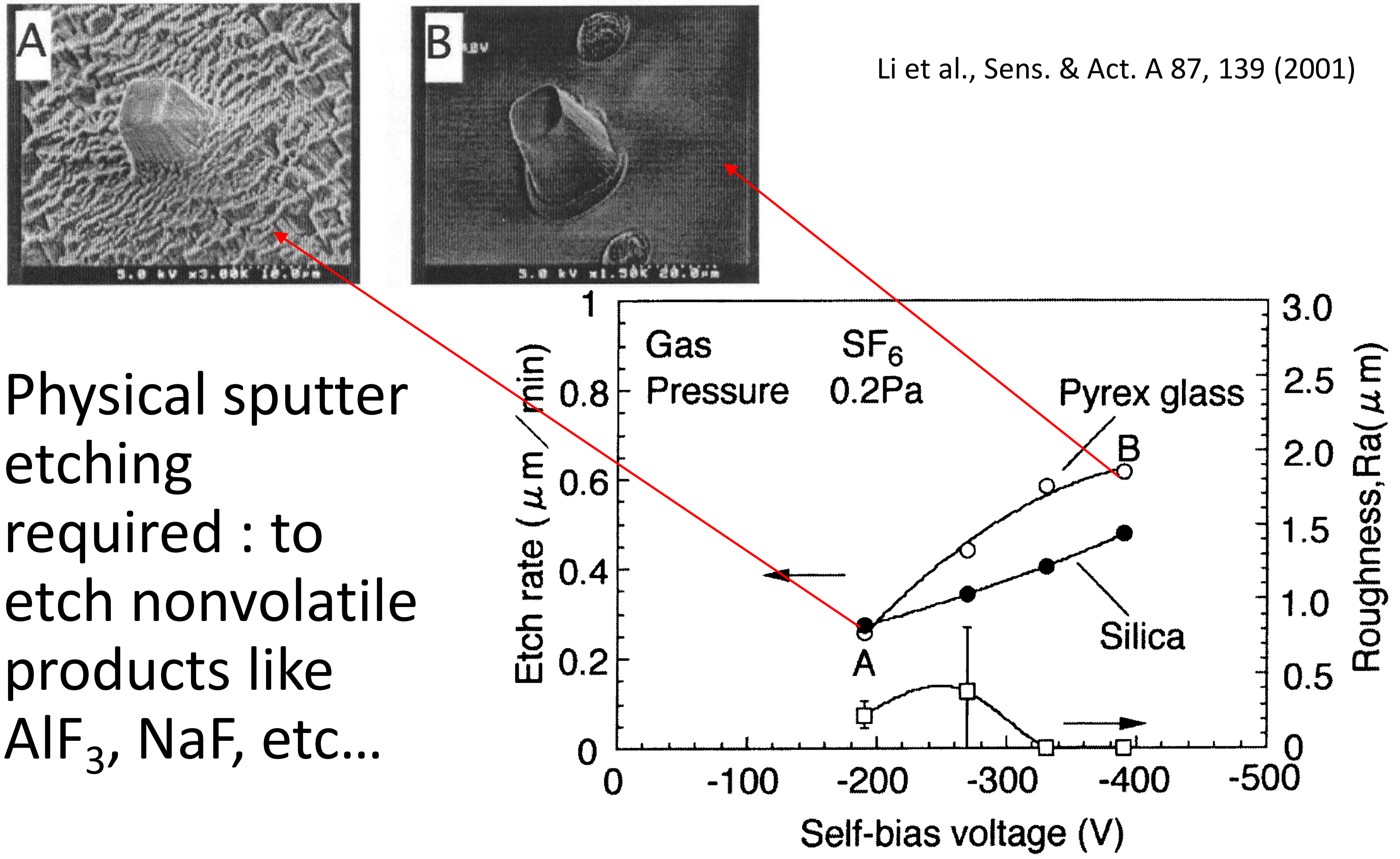

Fig. 4. Etch rates as a function of self-bias voltage and the SEM images (pressure 0.2 Pa, etching time 1 h).

Physical sputter etching required : to etch nonvolatile products like AlF_3, NaF, etc…

Multichannel Quartz Crystal Microbalance (QCM)

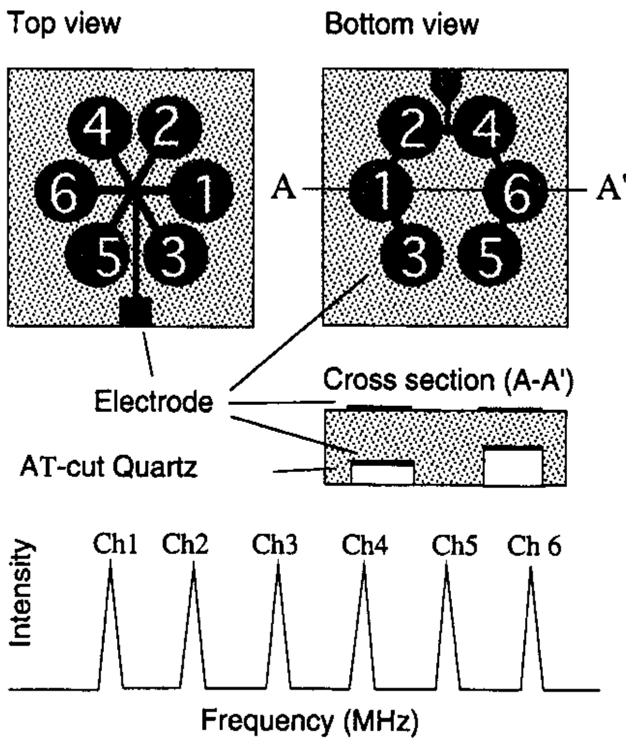

Fig. 1. Schematic illustration of idea of one-chip multichannel QCM sensor.

Abe et al., Sens. & Act. A 82, 139 (2000)

- AT-cut quartz crystal is piezoelectric material

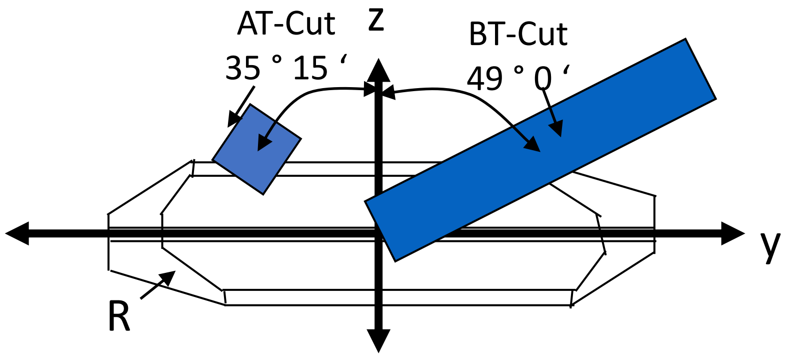

- Thickness shear mode vibration

- Resonance frequency depends on thickness

QCM process flow

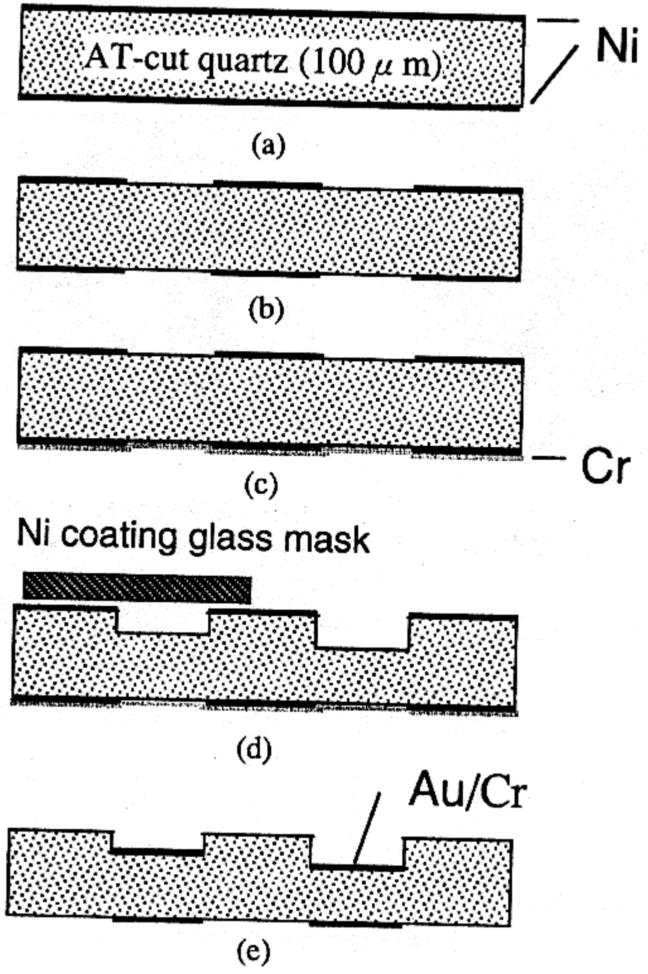

Fig. 2. Process steps of the multichannel sensor.

- SF_6 plasma (p = 0.2 Pa, self-bias = -340 V, T = 20 °C)
- Ni mask
- Selectivity Ni:quartz = 30

Abe et al., Sens. & Act. A 82, 139 (2000)

Influence of pressure

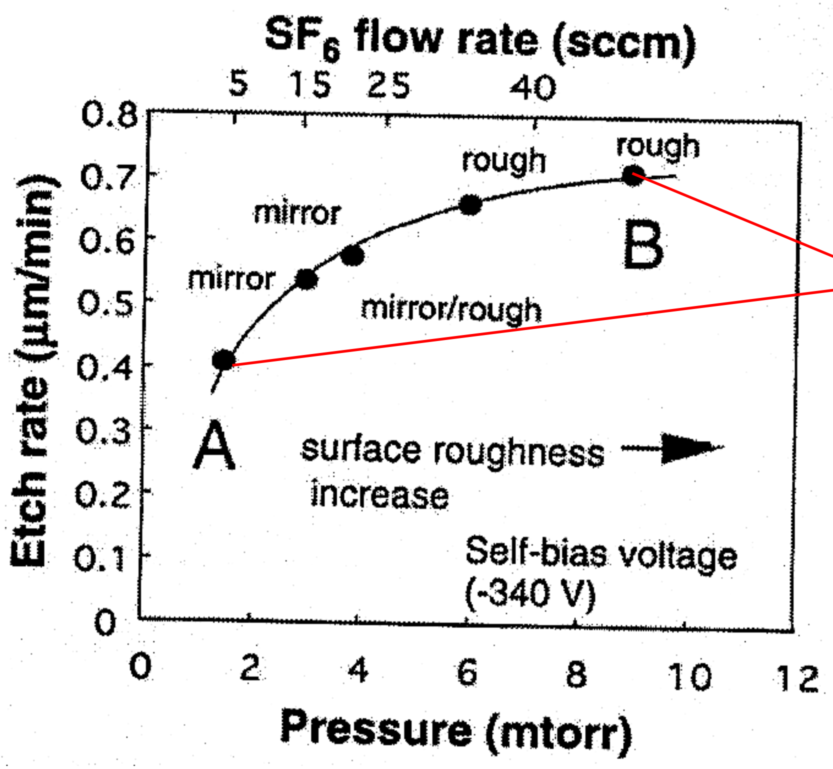

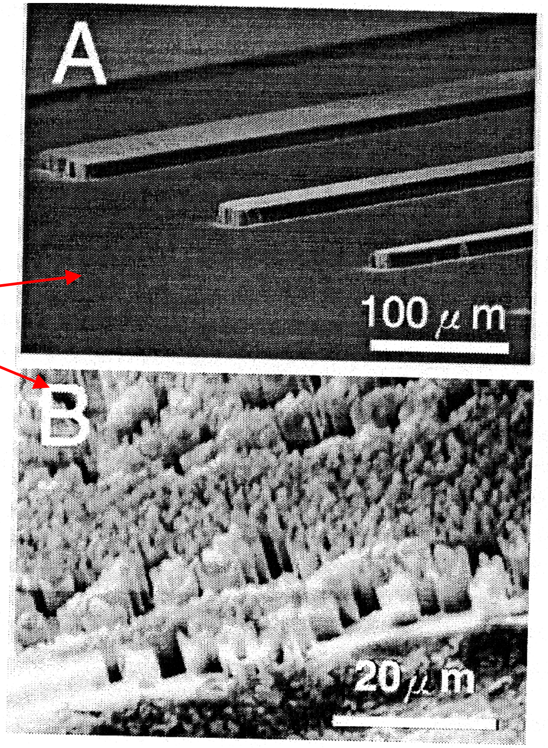

Fig. 3. Etch rate of AT-cut quartz as a function of process pressure and the SEM images (self-bias voltage, −340 V; etching time, 1 h; coil power, 150 W; cathode temperature, 20°C).

Abe et al., Sens. & Act. A 82, 139 (2000)

QCM sensor

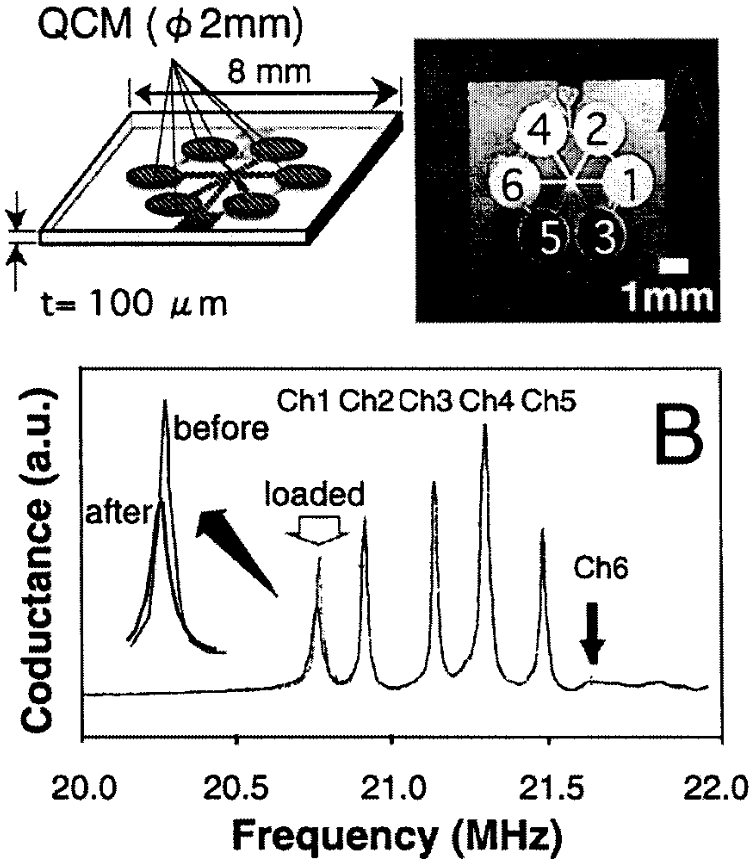

Fig. 6. Photograph of one-chip multichannel QCM sensor (A) and its resonant characteristics (B).

- f_{res} determined from conductance peak
- Diaphragm thickness : 77 → 81 μm
- f_{res} : 21.7 → 20.75 MHz
- Resolution for adsorbed mass : ± 1 ng (± 30 Hz)
- Application as odor sensor

Abe et al., Sens. & Act. A 82, 139 (2000)

References

- E. Gogolides, Ph. Vauvert, G. Kokkoris, G. Turban, A.G. Boudouvis, J. Appl. Phys. 88, 5570 (2000).
- X. Li, T. Abe, M. Esashi, Sens. & Act. A 87, 139 (2001).
- T. Abe, M. Esashi, Sens. & Act. A 82, 139 (2000).
- http://www.stsystems.com/
- http://www.alcatelvacuum.com/alcatel_avt/